

Direct surface analysis of time-resolved aerosol impactor samples with ultra-high resolution mass spectrometry

Stephen J. Fuller¹, Yongjing Zhao², Steven S. Cliff², Anthony S. Wexler², Markus Kalberer^{1}*

¹ University of Cambridge, Department of Chemistry, Lensfield Road, Cambridge, CB2 1EW,
UK

² Air Quality Research Center, University of California-Davis, Davis, California 95616, USA

ABSTRACT

Aerosol particles in the atmosphere strongly influence the Earth's climate and human health in urban areas but the quantification of their effects is highly uncertain. The complex and variable composition of atmospheric particles is the main reason for this uncertainty. About half of the particle mass is organic material, which is very poorly characterized on a molecular level and therefore it is challenging to identify sources and atmospheric transformation processes. We present here a new combination of techniques for highly time-resolved aerosol sampling using a rotating drum impactor (RDI) and organic chemical analysis using direct liquid extraction surface analysis (LESA) combined with ultra-high resolution mass spectrometry. This minimizes sample preparation time and potential artifacts during sample work up compared to conventional off-line filter or impactor sampling. Due to the high time resolution of about 2.5 hours intensity correlations of compounds detected in the high-resolution mass spectra were used to identify groups of compounds with likely common sources or atmospheric history.

INTRODUCTION

Aerosol particles are important components of the atmosphere and strongly influence the Earth's climate by directly scattering or absorbing sunlight and indirectly by aerosol-cloud interactions¹. Aerosol particles are also involved in negative health effects caused by air pollution and are linked to increases in respiratory and cardio-vascular diseases^{2,3}. All these particle effects are influenced by the chemical composition of the aerosol particles. A major fraction, often more than 50% in mass, of tropospheric aerosol is organic material, which is very poorly understood on a molecular level, although several thousand compounds have been separated with chromatographic techniques^{4,5}. To identify sources of particles but also to understand compositional changes during their atmospheric lifetime an automated method with high time resolution is highly desirable.

The analysis of the organic fraction of atmospheric aerosol particles on a molecular level is often challenging because their composition can be highly variable in time and space and usually only small sample amounts are available for analysis because atmospheric concentrations are typically a few micrograms per cubic metre⁶. The composition also depends on the size fraction of the aerosol, for example re-suspended, wind blown particles are mostly larger than 1 μm and have often a very distinct chemical composition compared to particles smaller than 1 μm , which are mainly emitted by combustion sources or formed by chemical reactions in the atmosphere⁶.

Thus, analytical-chemical techniques used to analyze atmospheric organic aerosol particles need to be highly sensitive to allow for highly time-resolved analyses at trace concentrations. In addition, the analysis technique needs to be able to characterize highly complex organic compound mixtures with thousands of mostly unknown components.

There are a number of analytical-chemical techniques that allow measuring the composition of aerosol particles with high time resolution. Online aerosol mass spectrometry (AMS) techniques⁷, for example, allow for very highly time-resolved particle composition studies. However, such measurements are demanding with respect to manpower and other resources and are usually performed only for a few weeks at a specific site. Thus, such measurements rarely provide insight into long-term trends of particle composition. In contrast, aerosol samples collected on filters or impactors over long time periods are more readily available, but have mostly a rather low time resolution of the order of a day or more and their chemical analysis usually involves time-consuming work up and is prone to artifacts during sample preparation.

The rotating drum impactor (RDI)⁸ is an offline sampling technique that allows for offline chemical analysis of particles with a time resolution on the hour time-scale^{9,10}, which is sufficient to resolve most atmospheric aerosol processes. The RDI has been combined with synchrotron X-ray fluorescence (s-XRF) analysis to measure changes in metal content directly from the RDI samples. Only one study analyzed so far organic components collected with a RDI^{11,12}: Emmenegger et al. (2004, 2005) investigated the temporal variability of polycyclic aromatic hydrocarbons collected at an urban location with two-step laser mass spectrometry, where an IR laser was used to desorb analytes directly from the RDI stripes without further sample preparation.

The recent development of commercially available surface mass spectrometry ionization techniques such as Liquid Extraction Surface Analysis (LESA)^{13,14} and Desorption Electro-Spray Ionisation (DESI)¹⁵ enables analysis of a wide range of organic compounds with high spatial and therefore high time resolution from RDI samples (for details see Method section). LESA has been used previously for the analysis of biological samples^{16,17} and pesticides¹⁸ but applications

for environmental samples have not yet been described in the literature. Another online extraction technique, Nano-DESI¹⁹, was recently presented by Roach et al. (2010) and was applied to atmospheric aerosol filter samples. Importantly LESA and (Nano-) DESI require no offline sample preparation, such as solvent extraction and solvent evaporation. Reducing the number of sample preparation steps also reduces the possibility of introducing artifacts.

For this study RDI collection was combined for the first time with LESA and ultra-high resolution mass spectrometry (UHR-MS) to characterize organic components in aerosol particles and to observe changes in ambient concentration with a time resolution of about 2.5 hours for sub- and super-micron particles. UHR-MS allows identification the elemental composition of unknown compounds and thus is a very valuable technique for the analysis of highly complex and often poorly characterized atmospheric organic aerosols where often the majority of the compounds are unknown.

EXPERIMENTAL SECTION

Sampling site location and sample collection

Rotating Drum Impactor (RDI) aerosol samples were collected at a site on the southern border of a dairy farm with about 1,200 milking cows in the San Joaquin valley in California, USA, one of the most intensively farmed regions in the US. The sampling site is discussed in more detail in the supporting information and in Zhao et al. (2012)²⁰.

A RDI, based on a design by Lundgren (1967)²¹, was used to collect size segregated aerosol samples for approximately 2 weeks from 11 am 25/5/2011 to 11 am 7/6/2011. The 4th generation RDI used in this study is described in detail in Zhao et al (2012)²⁰ and only a short description is

given here. Rather than collecting all particles on the same impaction spot during the sampling time, a Mylar strip on a slowly rotating drum is used as the impaction surface resulting in a time-resolved deposition of the impacted particles. Ambient air is sampled at a flow rate of 16.7 lpm and aerosol particles are collected via impaction on greased (Apiezon L high vacuum grease) Mylar strips. The Mylar is greased to increase the collection efficiency by reducing particle bouncing. The time resolution is determined by the rotation speed of the RDI drums combined with the aerodynamic spread of sample deposition. This varies with the particle size cut, with smaller particle sizes giving higher resolutions. The RDI sampler consists of 8 stages collecting samples in 8 size ranges (i.e., stage 1: 10-5, stage 2: 5-2.5, stage 3: 2.5-1.15 μm , stage 4: 1.15-0.75 μm , stage 5: 0.75-0.56 μm , stage 6: 0.56-0.34 μm , stage 7: 0.34-0.26 μm , and stage 8: 0.26-0.09 μm). Across all 8 stages the type of deposition could be divided visually into two distinct sample types, firstly on the stages collecting particles with larger diameters (stages 1 – 5), brown coloured particles follow a similar deposition variability with time. On stages with smaller diameter particles (stages 6 – 8) particle deposits were much darker and also showed a time variation similar to each other that was distinct from that observed on stages 1 – 5. Stage 3 and stage 8, corresponding to the size ranges 2.5-1.15 μm and 0.26-0.09 μm , respectively, were chosen as representative of the 2 deposition types and were investigated further in this study.

Sample analysis

The organic composition of particles deposited on stages 3 and 8 of the RDI were analyzed with mass spectrometry using a new direct extraction technique, Liquid Extraction Surface Analysis (LESA). LESA is a mode of operation of the TriVersa NanoMate chip-based nano electrospray ionisation (ESI) source (Advion, Ithaca, USA). Samples are mounted onto a

movable sample stage and a small amount of solvent (1 – 10 μL) is then dispensed from a pipette tip on the surface of the sample (Figure 1). The micro liquid junction is maintained to extract analytes present at (or close to) the surface of the sample and to dissolve them into the small solvent extraction volume. The droplet is aspirated and subsequently sprayed via an infusion method utilizing the chip based ESI²² (see supporting information). All mass spectra shown here were recorded in positive ionization mode.

A section of each Mylar RDI sample strip was cut to size (20 x 70 mm) and mounted on a standard glass microscope slide before being analyzed by LESA at 20 points along a linear path at 1 mm intervals, which corresponds to the approximate liquid junction droplet size as shown in Figure 2. This corresponds to a sampling start time of about 19:30 on 26th May 2011 and an end time of 21:50, 28th May 2011, with a sampling resolution of approximately 2 hours 40 minutes. Blank extractions were taken from an area at the edge of the strip where no sample was deposited. Extraction volumes of 1 μl of solvent (80:20 methanol:water) were deposited at a height of 0.8 mm from the sample surface to form the liquid junction which was maintained for 30 seconds. This time allowed for analytes present at or close to the surface of the RDI strips to dissolve. Only very limited loss of solvent and resolution was observed due to droplet spreading. Many previous studies using LESA have repeatedly deposited and aspirated solvent onto the sample on a single extraction spot to aid mixing of the extracted sample into the solvent within a short contact time of typically 1-5 seconds^{16,18,23}. However this leads to sample loss through each deposition/aspiration cycle as a small amount of solvent is lost to the surface each time the sample is aspirated. However a single deposition and aspiration reduces sample loss while increasing the contact time with the surface allows a longer period for analytes to dissolve²⁴, and

sufficient time for sample mixing through diffusion due to the small extraction volume. Contact times of over 30 seconds are less effective due to breakdown of the liquid junction.

An ultra-high-resolution mass spectrometer (LTQ Velos Orbitrap, Thermo Scientific, Bremen, Germany) with a resolution of 100,000 at m/z 400 and a typical mass accuracy of ± 2 ppm was used to analyze the organic compounds present in the samples following extraction by LESA. The resolution and mass accuracy of UHR-MS allows the identification of the elemental composition of unknown organic compounds. Samples were sprayed at a gas (N_2) pressure of 0.30 PSI at 1.8 kV in positive mode using a NanoMate Nano-ESI source.

FTMS data analysis

For each extraction point on the RDI stripes mass spectra were recorded for a one-minute infusion duration in a mass range of m/z 50-500. Almost no peaks above m/z 350 were detected and therefore only peaks below m/z 350 are discussed in the following. This mass range is a frequently observed characteristic of ambient aerosol composition²⁵. The instrument was calibrated to within ± 2 ppm using a standard calibration solution as prescribed by the manufacturer. Molecular formula were assigned within a ± 2 ppm error and within the following restrictions: Number of carbon atoms 1-20, C-13: 0-1, hydrogen = $0.2 \times C - 3 \times C$, oxygen = $0 - 3 \times C$, nitrogen = $0 - 1 \times C$, sulfate atoms = $0 - 1$, sodium atoms = $0 - 1$ and the following elemental ratios; $H/C = 0.2 - 3$, $O/C = 0 - 3$, $N/C = 0 - 1$. Peaks and assignments not following the nitrogen rule or containing C-13 were not considered further. In addition, peaks where no formula could be assigned within the restrictions mentioned above were also removed. Due to the low mass range of the detected peaks (below m/z 350) and the high accuracy of the instrument, multiple assignments are rare after considering the restrictions listed above. When

several formulae satisfied all restrictions within 2ppm, then the formula with the lowest mass error was assumed to be correct. Unfortunately due to the generally low peak intensities of the identified species MS-MS analysis for further structural identification was not possible. Only about 10-15% of the peaks contain a sulfur atom and are not further discussed here. See supporting information for more details on the data analysis procedure.

For both stage 3 and 8, two blanks were taken from unused areas of the Mylar strip for which only grease was present. The mass spectra from these blanks were processed following the same method as the samples. Any molecular formula identified in both the sample and either of the blanks from the same stage were deleted regardless of intensity. Approximately 50% of the formula from stage 3 and 75% from stage 8 were also present in the greased blank. The grease present on the stripes is hydrocarbon based and so is not ionized by electro-spray ionization. Thus, compounds detected in the blank spectra are likely due to impurities in the grease or oxidation products of its components, leading to a high chemical background. The large chemical background might have affected analyte ionization efficiencies but assuming these matrix effects are constant on the entire sample this should not affect significantly the results of this study.

The final list of assigned peaks contained about 950 formulae for stage 3 and 720 formulae for stage 8. Despite the large number of peaks in the background due to the grease used during the sample collection, clear trends could be identified over the two-day sampling time analyzed in this study, as discussed below.

RESULTS AND DISCUSSION

Sample loading and meteorological data

The two sample Mylar strips analyzed here are shown in Figure 2. For stage 3 (Figure 2.a), 2 separate types of deposit were identified visually. Firstly, three brown coloured regions (labeled as 'A') that show a maximum loading on extraction points 1/2, 9/10 and 17. Secondly, a light coloured (labeled as 'B') deposition with maximum loadings on extraction points 3, 4 and 13. Stage 8 (Figure 2.b) shows generally a much darker deposit colour with pronounced dark deposit between extraction points 2 and 3, and slightly dark areas on extraction points 9, 10, 18 and 20.

The meteorological data collected at the nearby airport shows the wind direction is from the northwest for the entire duration of the 2-day sampling period. The wind speed however is more variable with three periods of higher wind speeds between 12:00 and 00:00 each day during the sampling period, showing a maximum of 28 kmph. The wind speed is plotted in Figure 3 and compared to the sample loading, which was quantified by taking the grey levels from a bitmap file of the grey-scale scanned image of each sample strip. These were scaled to values between 0 and 1 and reflect the visual inspection of the loading: for stage 3 the lightest areas (i.e., A and B type deposits) corresponded to the highest loading and extraction spot 1 was assigned a value of 1, and thus the darkest areas were assigned a value of zero (extraction point 7 and 15) and the other values scaled linearly. The opposite scaling was used for stage 8, where darker regions indicate higher loading. The dark colour is possibly due to increased amounts of elemental carbon on the stripe. The periods of high wind speed correlate reasonably well with the higher loadings on stage 3 of the A type deposit, which suggests that this is wind blown dust from the local area. However no links could be made between the B type deposits and the meteorological data. Periods with an increased sample loading on stage 8 appears to occur at night, suggesting

that this may be due to diurnal changes in the boundary layer height concentrating sub-micron particles during the night in the shallow boundary layer.

Elemental ratios of organic compounds

Average intensity weighted molecular formula were identified for each stage (see Table 1). The overall average composition for the entire mass range up to m/z 350 is similar between the two stages. However in the mass range $< m/z$ 200 stage 3 has an O/C ratio which is 50% larger (0.34) than the O/C ratio of stage 8 (0.23). Differences in the N/C ratio between the two stages are smaller than the O/C ratio. About 40% of all compounds on both stages contain only C, H and O atoms and about 12% (stage 3) and 19% (stage 8) contain only C, H and N. About 30-35% of all compounds contain C, H, O and N.

Figure 4 shows the O/C and N/C ratios of the most intensive peaks in the mass spectra as a function of their molecular mass from both stages. For clarity only the most intensive 200 peaks in the mass spectra are shown here, which correspond to about 80% of the total ion intensity. The molecular formulae from all 20 extraction points were combined and their intensities from each point summed. Stage 3 is shown in blue and stage 8 in red, superimposed on top of the stage 3 data. The elemental ratios of O/C and N/C ratio were found to vary with particle size fraction (between the stages) and with molecular mass range.

Figure 4a shows 15% more compounds containing only C, H and O among the 200 most abundant species in stage 3 than stage 8 (165 compounds compared to 141). For these CHO species in stage 3, 69% of the top 200 peaks by number and 87% by intensity have a neutral mass of <200 Da. In comparison for stage 8 only 57% by number and 45% by intensity are in this mass range. This is due to a larger number of compounds in stage 8 with no oxygen content,

but only C, H and N indicating the presence and importance of amine type species in this sub-micron particle size range. The similarity of the nitrogen content between the stages is due to this increased abundance of CHN compounds in stage 8 being balanced by the presence of more oxidized nitrogen species (CHNO) in stage 3. Figure 4b shows that the nitrogen content is largely similar for both stages, however for stage 3 for a neutral mass of <200 Da a large number of high intensity compounds are present on the baseline with a N/C ratio of zero, indicating that they contain only C, H and O, which is accordance with the higher O/C ratio in the bulk composition in the same mass range (Table 1).

For all compounds below m/z 150 (181 compounds) in the large size fraction (stage 3) the N/C ratio is clearly correlated with the overall particle loading and wind speed (Figure S2). This strongly suggests that compounds in the low mass region with high nitrogen content may be soil derived. Soil organic compounds are known to have a large number of N-containing compounds²⁶. The sampling location close to a dairy farm could also partly explain the high N/C ratio of the large particle fraction under high wind conditions, due to the high N-content of animal waste. This correlation is not as strong if all compounds up to m/z 350 are considered.

Kendrick mass defect analysis

To further characterize the compounds in the two stages Kendrick mass defect plots were constructed. The Kendrick mass scale assigns an integer mass of 14.000 to CH_2 in place of the IUPAC mass of 14.0156 for all compounds (see supporting information for more detailed definition). Compounds with the same number of hetero-atoms and double bond equivalents will have the same KMD and differ by a KM of 14 if their formula differs by a CH_2 group only, defined here as KMD-series. This is used to identify possible homologous aliphatic series, which

will appear on a horizontal line when KMD is plotted against nominal mass²⁷. However without structure confirmation by MS/MS analysis or otherwise these series do not necessarily have structural similarity in complex samples such as organic aerosols.

Figure 5 shows KMD plots of all CHN and CHO compounds for both stages that fall into KMD-series with more than three species. There were a significantly greater number of CHN series present in stage 8 (60 compounds, Figure 5b) than in stage 3 (28 compounds, Figure 5a) and similarly more CHO series in stage 3 (151 compounds, Figure 5c) than in stage 8 (60 compounds, Figure 5d) confirming the findings discussed above (Table 1 and Figure 4).

Intensity correlations

It is often assumed in that such KMD-series of compounds are structurally related may thus originate from the same source. Structurally closely related compounds, especially when emitted from the same source, often have similar atmospheric lifetimes due to similarities in reactivity. Thus their concentrations may be strongly correlated with each other over time. The high time resolution of the RDI dataset allows the evaluation of such a hypothesis. Figure 6a shows the change of intensity with time of compounds identified in a series with four members starting with a core molecule of formula $C_5H_8N_2$ found on stage 8. It can be seen here that all four members show high intensities on spots 12-15 and the two first members are also strongly correlated over the entire measurement time. This suggests that these species are associated with the same source and strengthens the argument that they may be structurally related. In Figure 6b, the same analysis of a series with four members starting with $C_7H_{10}O_3$ present on stage 3 shows no relationship between the individual compounds of the series over the entire sampling time, indicating it is less likely that they are related by source or structure.

The five KMD-series of each stage with on average the most intensive ions are listed in Table 2, with the core molecule being the molecule with the smallest mass in the series and the $(\text{CH}_2)_n$ -number describing the number of CH_2 units in addition to the core molecule. Four of these five series in stage 3 are compounds consisting of only CHO where as all five series in stage 8 contain nitrogen atoms. Most N-containing compounds have no or only a small number of oxygen atoms and are therefore likely to be amines, which are favorably ionized in positive mode mass spectrometry. Reduced nitrogen containing KMD-series have been identified previously as biomass burning markers in aerosols²⁸. Thus, also in the samples analyzed here some CHN series in the sub-micron size fraction could originate from biomass burning sources. This marked difference between the two stages mirrors the bulk elemental O/C and N/C ratios discussed previously, with stage 3 containing more oxygenated species and stage 8 more amines.

As shown above it is often difficult to identify groups of compounds originating from a common source and correlations of peak intensities over time allow the possible identification of compounds with a common or similar atmospheric history. Thus, for each identified formula the variation of intensity across the 20 sampling points was compared to every other formula in the entire data set. Linear regression analysis was used to indicate correlations, and any correlation with an R^2 value of greater than 0.8 were defined as statistically significant. This analysis assumes that matrix ionization effects are constant throughout the RDI stripe due to the hydrocarbon grease applied to the Mylar strips. This resulted in a number of sets of correlating species for stage 3. Three of these correlating sets of species are shown in Table S1, which gives for each set the formula and the total peak intensities across all twenty extraction points. Figure 7 shows the variation in the averaged intensity for all the species in each set for each extraction point, which was subsequently normalized to the maximum average intensity across all 3 series

of correlating species and across all extraction points. Series 1 contains both CHNO and CHN species and series 2 contains only CHO compounds. Both series show a negative correlation to the brown-coloured regions in stage 3 (Figure 2a). In contrast, series 3 contains CHNO compounds only and shows a positive correlation with the brown deposit (extraction points 9/10 and 17, Figure 2a). Series 3 also correlates with the overall N/C ratio and wind speed as shown in Figure S2, again suggesting that these compounds may be soil derived and from local (farm) sources. No series of correlating species were identified by this method in stage 8 indicating a more complex composition and atmospheric history of the small particle fraction.

CONCLUSIONS

We developed a new technique to analyze the organic composition of atmospheric aerosol on a molecular level with a high time resolution by combining a new extraction and ionization technique, LESA, with RDI samples and ultra-high resolution mass spectrometry. LESA facilitates analysis without time-consuming sample preparation or extraction and also allows direct extraction from a sample surface with high spatial resolution, which when combined with RDI samples results in highly time-resolved information of ambient aerosol organic content.

Ultra-high resolution mass spectrometry was used to determine the chemical composition of organic compounds and to investigate their changes in intensity over the sampling period in two aerosol size ranges. Changes in the chemical composition could be related to changes in meteorological conditions, for example the signal intensity of a subset set of nitrogen-containing compounds was found to be associated with the local wind-speed suggesting that these compounds are largely of local origin. Groups of compounds were identified that showed similar trends in abundance over the sampling period indicating that these compounds originate from the

same source. This was demonstrated by the identification of homologous series, which are likely associated with biomass burning sources. A further characterization of the structures of the compounds, e.g., by performing MS-MS experiments, was not possible due to the generally low peak intensities. This could be overcome in future studies by a lower rotation speed of the RDI during sample collection, which would allow for higher sample loadings and might allow sufficient peak intensities to perform MS-MS experiments.

While mass spectrometry is widely used to identify organic aerosol content, the combination with LESA and RDI sampling allows a much higher temporal sampling resolution than would be possible with other offline techniques allowing to identify marker compounds and to follow atmospheric processes in detail.

AUTHOR INFORMATION

Corresponding Author

* email: markus.kalberer@atm.ch.cam.ac.uk, phone: +44 1223 336392, fax: +44 1223 336362

Notes

The authors declare no competing financial interest.

ACKNOWLEDGMENTS

Financial support by the UK Natural Environment Research Council (NERC), project NE/H52449X/1 and by Advion Bioscience LTD via a CASE Award is greatly acknowledged.

REFERENCES

- (1) Seinfeld, J. H.; Pandis, S. N. *From Air Pollution to Climate Change.*; John Wiley and Sons, New York, **1998**; p. 1326.
- (2) Brunekreef, B.; Holgate, S. T. *The Lancet* **2002**, *360*, 1233-1242.
- (3) Breyse, P. N.; Delfino, R. J.; Dominici, F.; Elder, A. C. P.; Frampton, M. W.; Froines, J. R.; Geyh, A. S.; Godleski, J. J.; Gold, D. R.; Hopke, P. K.; Koutrakis, P.; Li, N.; Oberdörster, G.; Pinkerton, K. E.; Samet, J. M.; Utell, M. J.; Wexler, A. S. *Air Qual., Atmos. Health* **2012**, Submitted.
- (4) Schnelle-Kreis, J.; Welthagen, W.; Sklorz, M.; Zimmermann, R. *J. Sep. Sci.* **2005**, *28*, 1648-1657.
- (5) Sheesley, R. J. *J. Geophys. Res.* **2003**, *108*, 4285; DOI:10.1029/2002JD002981. .
- (6) Pöschl, U. *Angew. Chem., Int. Ed. Eng.* **2005**, *44*, 7520-40.
- (7) Jayne, J.; Leard, D.; Zhang, X.; Davidovits, P.; Smith, K.; Kolb, C.; Worsnop, D. *Aerosol Sci. Technol.* **2000**, *33*, 49-70.
- (8) Raabe, O. G.; Braaten, D. a; Axelbaum, R. L.; Teague, S. V.; Cahill, T. A. *J. Aerosol Sci.* **1988**, *19*, 183-195.
- (9) Richard, A.; Bukowiecki, N.; Lienemann, P.; Furger, M.; Fierz, M.; Minguillón, M. C.; Weideli, B.; Figi, R.; Flechsig, U.; Appel, K.; Prévôt, a. S. H.; Baltensperger, U. *Atmos. Meas. Tech.* **2010**, *3*, 1473-1485.

- (10) Bukowiecki, N.; Lienemann, P.; Hill, M.; Figi, R.; Richard, A.; Furger, M.; Rickers, K.; Falkenberg, G.; Zhao, Y.; Cliff, S. S.; Prevot, A. S. H.; Baltensperger, U.; Buchmann, B.; Gehrig, R. *Environ. Sci. Technol.* **2009**, *43*, 8072-8.
- (11) Emmenegger, C.; Kalberer, M.; Samburova, V.; Zenobi, R. *Analyst* **2004**, *129*, 416-20.
- (12) Emmenegger, C.; Kalberer, M.; Samburova, V.; Zenobi, R. *Environ. Sci. Technol.* **2005**, *39*, 4213-9.
- (13) Kertesz, V.; Ford, M. J.; Berkel, G. J. Van *Anal. Chem.* **2005**, *77*, 7183-9.
- (14) Kertesz, V.; Berkel, G. J. Van *J. Mass Spectrom.* **2010**, *45*, 252-60.
- (15) Takáts, Z.; Wiseman, J. M.; Gologan, B.; Cooks, R. G. *Science* **2004**, *306*, 471-3.
- (16) Eikel, D.; Vavrek, M.; Smith, S.; Bason, C.; Yeh, S.; Korfmacher, W. a; Henion, J. D. *Rapid Commun. Mass Spectrom.* **2011**, *25*, 3587-96.
- (17) Edwards, R. L.; Creese, A. J.; Baumert, M.; Griffiths, P.; Bunch, J.; Cooper, H. J. *Anal. Chem.* **2011**, *83*, 2265-2270.
- (18) Eikel, D.; Henion, J. *Rapid Commun. Mass Spectrom.* **2011**, *25*, 2345-2354.
- (19) Roach, P. J.; Laskin, J.; Laskin, A. *Analyst* **2010**, *135*, 2233-6.
- (20) Zhao, Y.; Cliff, S. S.; Wexler, A. S.; Perry, K.; Pan, Y.; Mitloehner, F. M. *Atmos. Environ.* **2012**, Submitted.
- (21) Lundgren, D. A. *Journal of the Air Pollution Control Association* **1967**, *17*, 225-9.
- (22) Schultz, G. A.; Corso, T. N.; Prosser, S. J.; Zhang, S. *Anal. Chem.* **2000**, *72*, 4058-4063.

- (23) Paine, M. R. L.; Barker, P. J.; Maclaughlin, S. a; Mitchell, T. W.; Blanksby, S. J. *Rapid Commun. Mass Spectrom.* **2012**, *26*, 412-8.
- (24) Walworth, M. J.; ElNaggar, M. S.; Stankovich, J. J.; Witkowski, C.; Norris, J. L.; Berkel, G. J. Van *Rapid Commun. Mass Spectrom.* **2011**, *25*, 2389–2396.
- (25) Rincon, A. G.; Calvo, A. I.; Dietzel, M.; Kalberer. M. *Environ. Chem.* **2012**, *9*, 298-319.
- (26) Knicker, H. *Soil Biol. Biochem.* **2011**, *43*, 118-1129.
- (27) Kendrick, E. *Anal. Chem.* **1963**, *35*, 2146-2154.
- (28) Laskin, A.; Smith, J. S.; Laskin, J. *Environ. Sci. Technol.* **2009**, *43*, 3764-71.

TABLES

Table 1. Average molecular formula and average elemental ratios of all assigned formulas.

	Av. molecular formula	N/C	O/C
Stage 3 < m/z 200	$C_{6.6}H_{11.0}N_{1.0}O_{2.2}$	0.15	0.34
Stage 3 < m/z 350	$C_{7.5}H_{12.2}N_{1.4}O_{2.3}$	0.19	0.30
Stage 8 < m/z 200	$C_{6.8}H_{12.1}N_{1.3}O_{1.6}$	0.19	0.23
Stage 8 < m/z 350	$C_{8.7}H_{15.5}N_{1.4}O_{2.5}$	0.16	0.28

Table 2. Kendrick mass defect (KMD) series with the highest average peak intensities identified in stages 3 and 8.

Core molecule	DBE	(CH ₂)n, Stage 3	(CH ₂)n, Stage 8
<u>Stage 3</u>			
C ₃ H ₈ O ₃	0	0, 2, 7, 8, 13	- *
C ₄ H ₄ O ₂	3	0-4, 6, 8, 9	-
C ₂ H ₆ O ₂	0	0-2, 4, 6	-
C ₆ H ₁₃ N	1	0-3	0-2, 9
C ₃ H ₄ O ₄	2	0-2, 4, 7, 8, 13	-
<u>Stage 8</u>			
C ₄ H ₁₁ NO	0	-	0, 2, 4, 10, 12
C ₅ H ₈ N ₂	3	0-3	0-8
C ₄ H ₉ NO ₂	1	-	0, 3-5
C ₉ H ₂₁ N	0	-	0, 2, 3, 6, 10
C ₇ H ₆ N ₂	6	-	0-7

* : series not present in this sample.

FIGURES

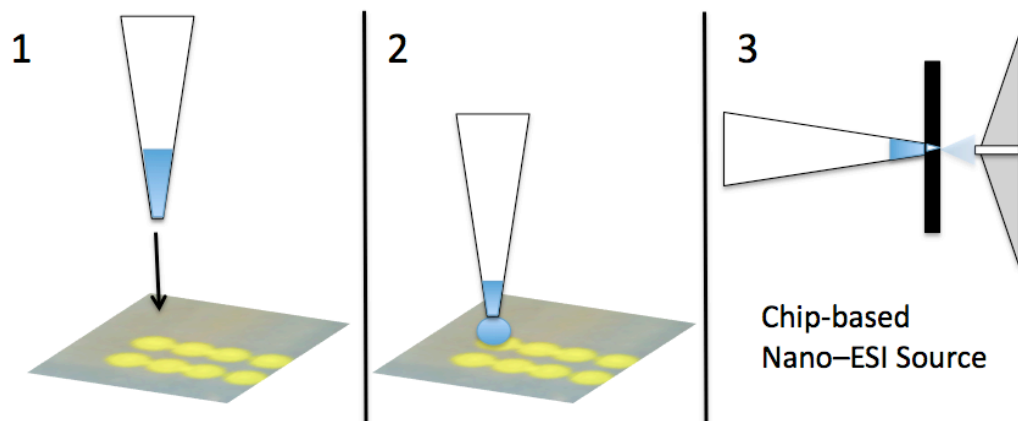


Figure 1. Schematic of the Liquid Extraction Surface Analysis (LESA) technique. (1) A pipette tip containing the extraction solvent is brought very close to the samples surface. (2) 1 μ l solvent is then dispensed onto the sample surface, while a liquid junction is maintained. Chemical compounds present at or near the surface of the sample are extracted into the small solvent droplet. (3) After aspirating the extraction solvent back into the pipette tip, the extract is analyzed with a mass spectrometer via a nano-EI source.

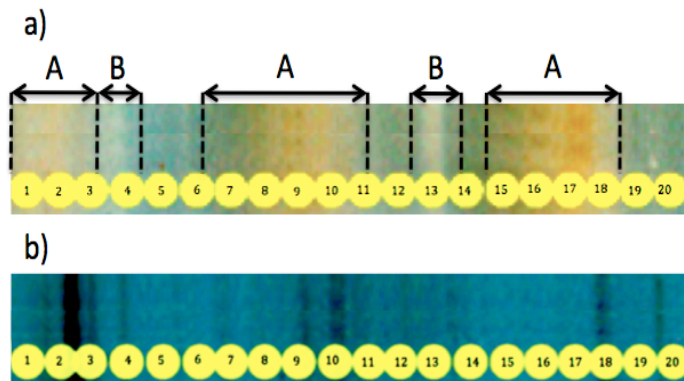


Figure 2. Scanned images of Rotating Drum Impactor (RDI) stage 3 (a) and stage 8 (b) showing time-resolved deposition of the particles with different types of sample colour and loading.

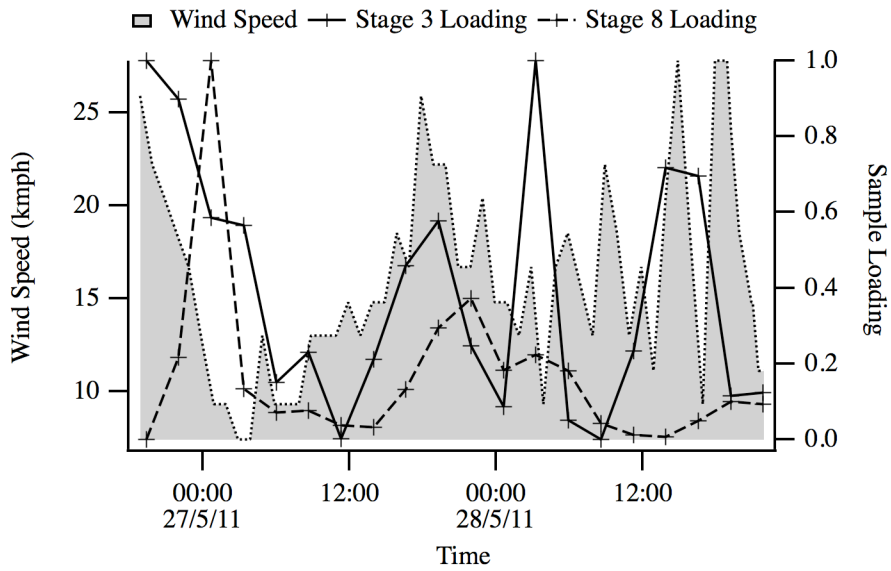


Figure 3. Wind speed (left y-axis) compared with sample loading as quantified from the grey-scale image intensity (right y-axis) for all 20 sample points and both RDI stages 3 and 8.

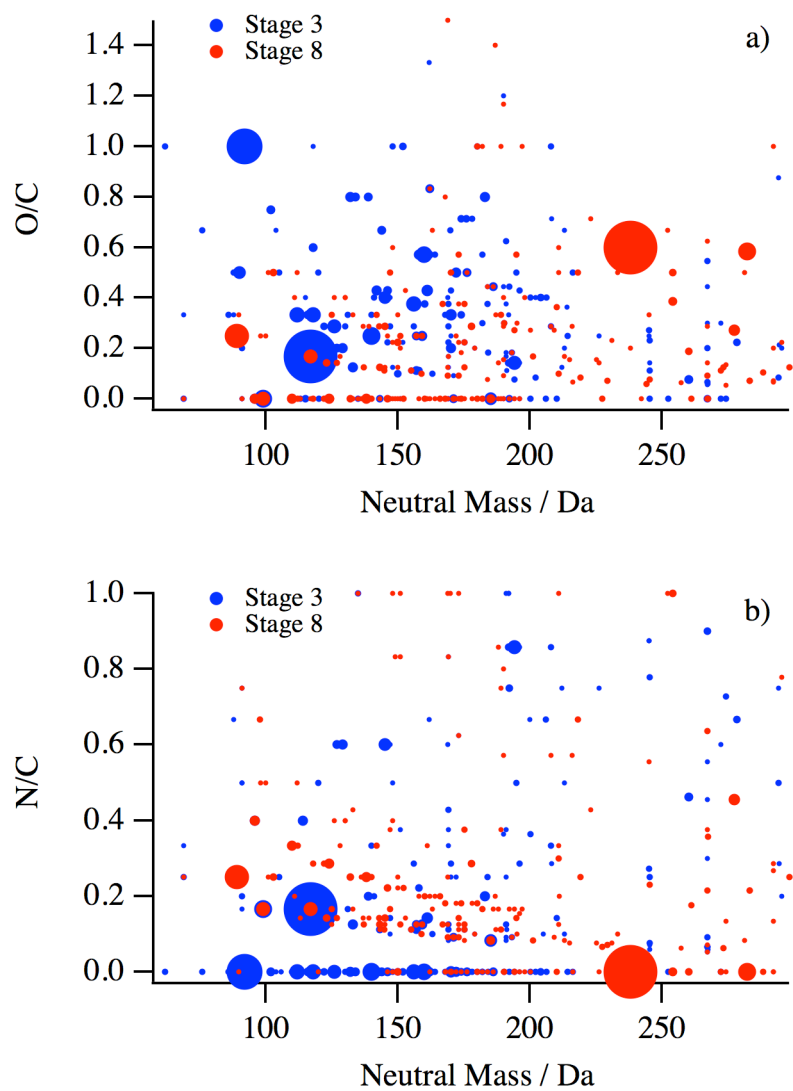


Figure 4. Elemental ratios of formulas for the most intense 200 peaks in the mass spectra in both stages (3 and 8) as a function of their neutral mass. (a) Shows O/C ratio and (b) N/C ratio. Symbol size reflects peak intensity

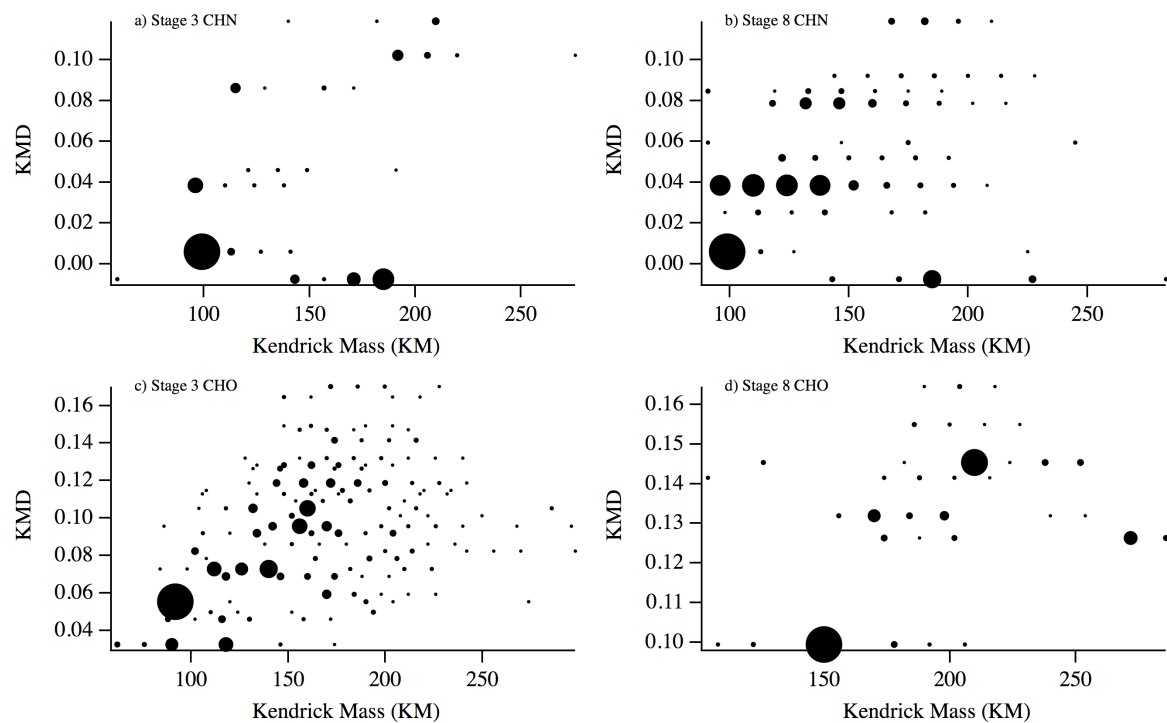


Figure 5. Kendrick mass defect (KMD) against Kendrick mass for CHN and CHO compounds in stage 3 and 8 for all compounds that fall into KMD-series with more than three members.

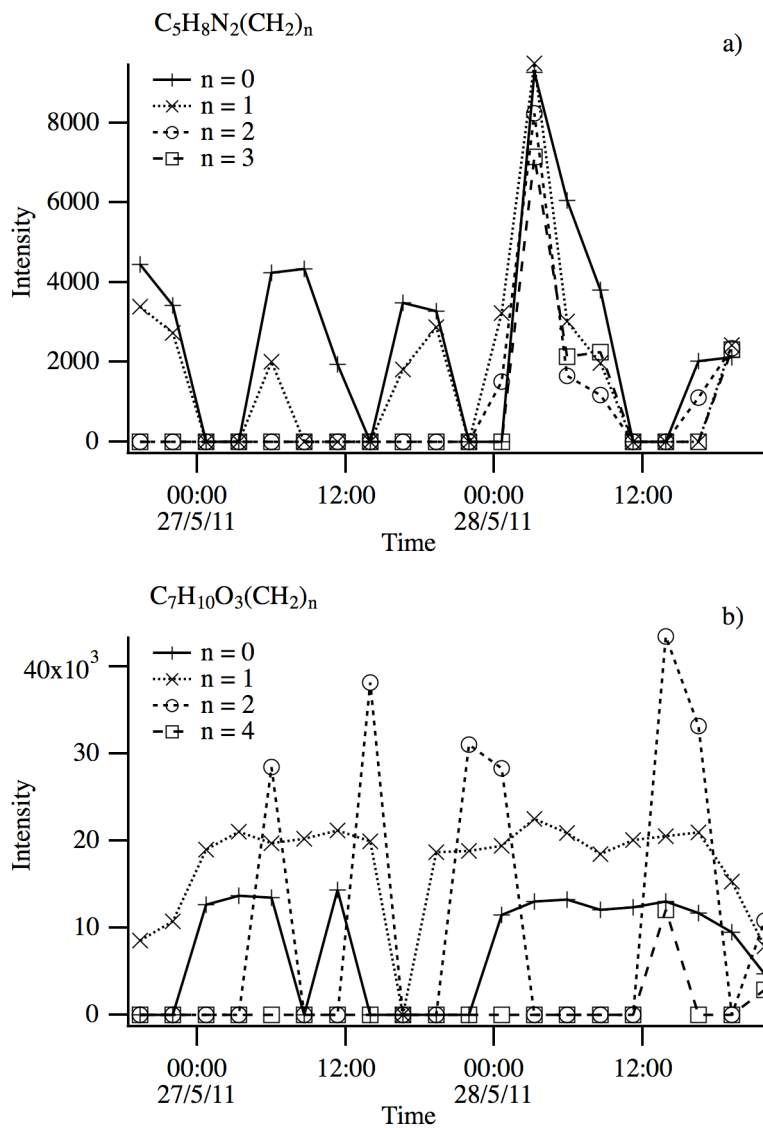


Figure 6. (a) The intensities of the compounds from the same KMD-series based on a $C_5H_8N_2$ core are correlated over time. (b) The same analysis shows that for other KMD-series no such correlation is found between members, as exemplified here with a series based on a $C_7H_{10}O_3$ core.

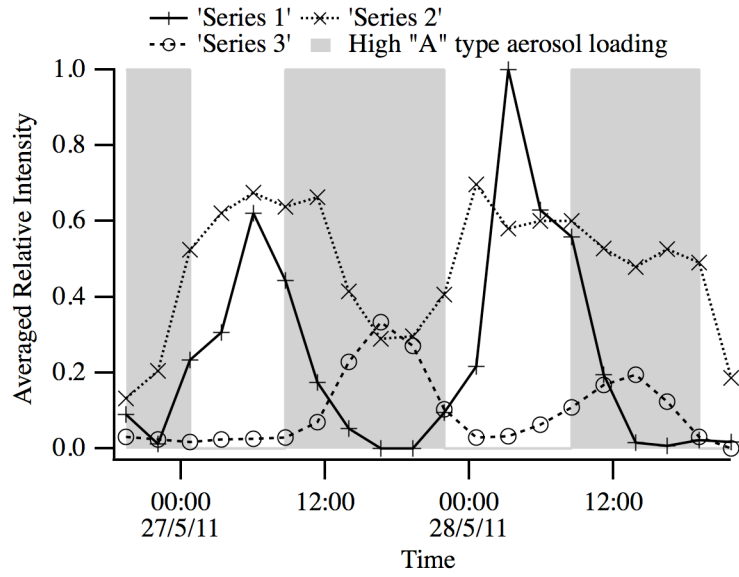


Figure 7. Relative intensity variations for the three identified sets of compounds in stage 3 as listed in Table 3. Time periods with intensive brown-coloured particle deposits (See Figure 2a), which are likely from soil-derived local sources, are indicated with solid bars.